Formation of Stimuli-Responsive Supramolecular Polymeric Assemblies *via* Orthogonal Metal–Ligand and Host–Guest Interactions

*Yue Ding, Peng Wang, Yu-Kui Tian, Yu-Jing Tian and Feng Wang**

Key Laboratory of Soft Matter Chemistry,
Department of Polymer Science and Engineering,
University of Science and Technology of China,
Hefei, Anhui 230026 (P. R. China)
Fax: (+86) 551 3606 095; E-mail: drfwang@ustc.edu.cn.

Supporting Information

1. Materials and methods

N-(3-dimethylaminopropyl)-*N*′-ethylcarbodiimide hydrochloride (EDC·HCl), 4-dimethylamino pyridine (DMAP), sodium borohydride ($NaBH_4$), terephthalic acid, *n*-butylamine, NH_4PF_6 and zinc triflate ($Zn(OTf)_2$) were reagent grade and used as received. 4'-(*p*-hydrophenyl)-2,2':6',2"-terpyridine **6**,[S1] 4-(10-bromodecyloxy)benzaldehyde **7**[S2] and B21C7 alcohol **9**[S3] were synthesized according to the literature procedures. Other reagents and solvents were employed as purchased.

NMR spectra were collected on a Varian Unity INOVA-300 spectrometer with TMS as the internal standard. Electrospray ionization mass spectra (ESI-MS) were obtained on a Bruker Esquire 3000 plus mass spectrometer (Bruker–Franzen Analytik GmbH Breman, Germany) equipped with an ESI interface and an ion trap analyzer. Viscosity measurements were carried out with Ubbelohde dilution viscometers (Shanghai Liangjing Glass Instrument Factory, 0.47 mm inner diameter) in chloroform/acetonitrile (3/1, *v/v*) containing 0.05 M tetrabutylammonium hexafluorophosphate to exclude the polyelectrolyte effect. UV/Vis spectra were recorded on a Beijing Persee TU-1901 UV-Vis spectrometer.

*2. Synthetic routes to the desired compounds **1** and **2***

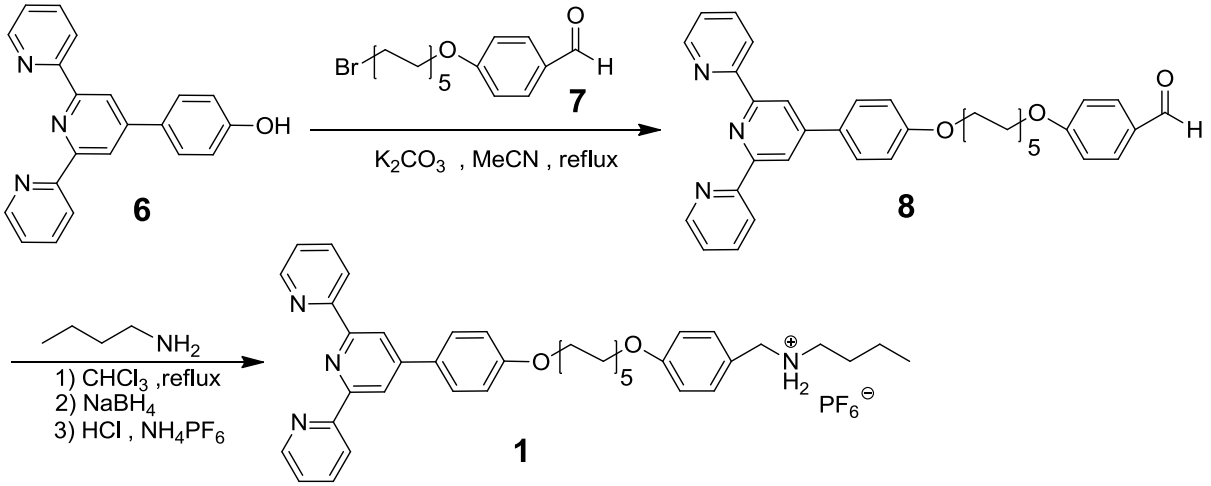

Scheme S1. Synthesis of the heteroditopic monomer **1**.

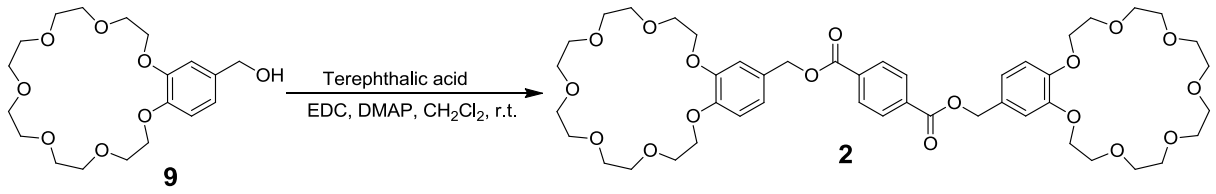

Scheme S2. Synthesis of the homoditopic B21C7 host **2**.

*2.1 Synthesis of compound **8***

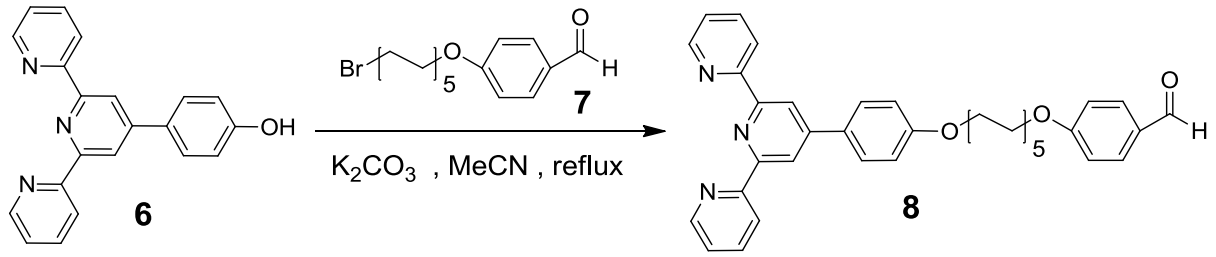

Compounds **7** (2.62 g, 7.38 mmol), **6** (2.00 g, 6.15 mmol) and K_2CO_3 (2.00 g, 14.5 mmol) were refluxed in acetonitrile (100 mL) for 12 h. After filtration of K_2CO_3, the solvent was removed with a rotary evaporator and the residue was extracted with H_2O/CH_2Cl_2. The combined organic extracts were then removed with a rotary evaporator. Subsequently, the residue was purified by flash column chromatography (dichloromethane/methanol, 12 : 1 *v/v* as the eluent) to afford compound **8** as a pale yellow liquid (2.48 g, 67%). The ^{1}H NMR spectrum of compound **8** is shown in Figure S1. ^{1}H NMR (300 MHz, $CDCl_3$, room temperature) δ (ppm): 9.87 (s, 1H), 8.68 (m, 6H), 7.86 (m, 6H), 7.35 (m, 2H), 7.00 (m, 4H), 4.03 (s, 4H), 1.82 (m, 4H), 1.47 (m, 4H), 1.36 (m, 8H). The ^{13}C NMR spectrum of compound **8** is shown in Figure S2. ^{13}C NMR (75 MHz, $CDCl_3$, room temperature) δ (ppm): 190.9, 164.4, 160.3, 156.6, 156.0, 150.0, 149.3, 137.0, 132.0, 130.7, 129.9, 128.6, 123.9, 121.5, 118.4, 115.0, 68.6, 68.2, 29.6, 29.5, 29.4, 25.9. ESI–MS m/z: $[M + H]^+$ calcd for $C_{38}H_{40}N_3O_3$, 586.3070; found, 586.3045; error, 4.3 ppm.

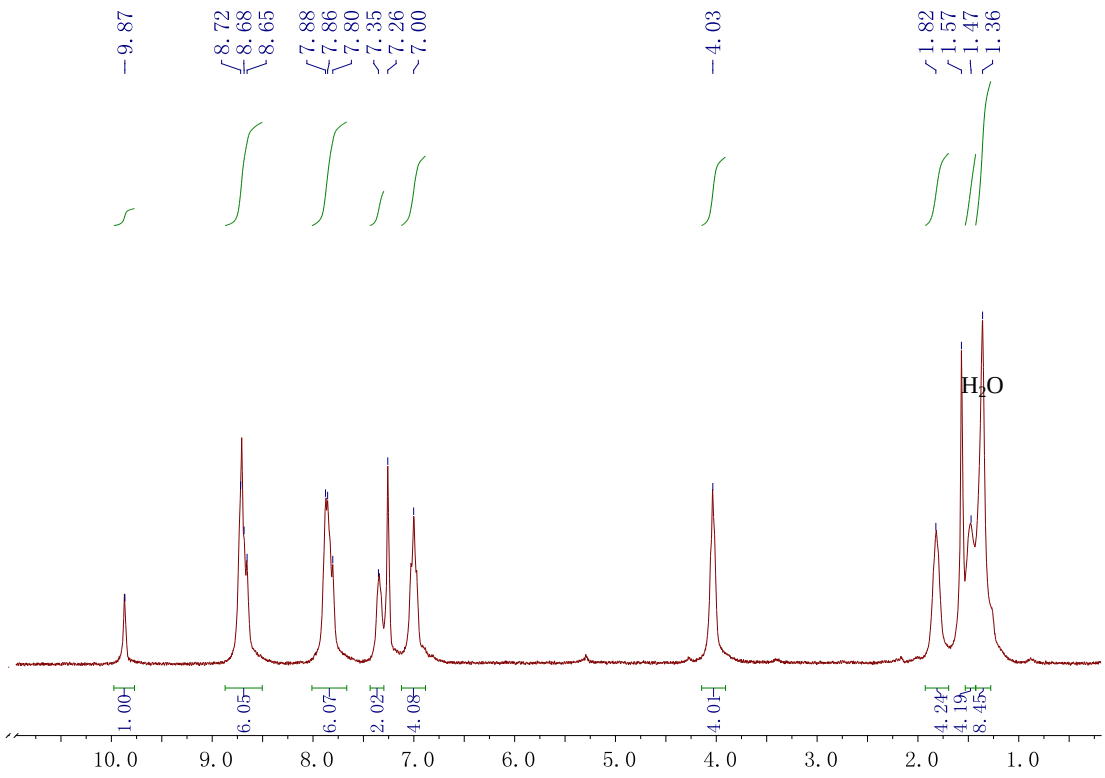

Figure S1. ^{1}H NMR spectrum (300 MHz, $CDCl_3$, room temperature) of compound **8**.

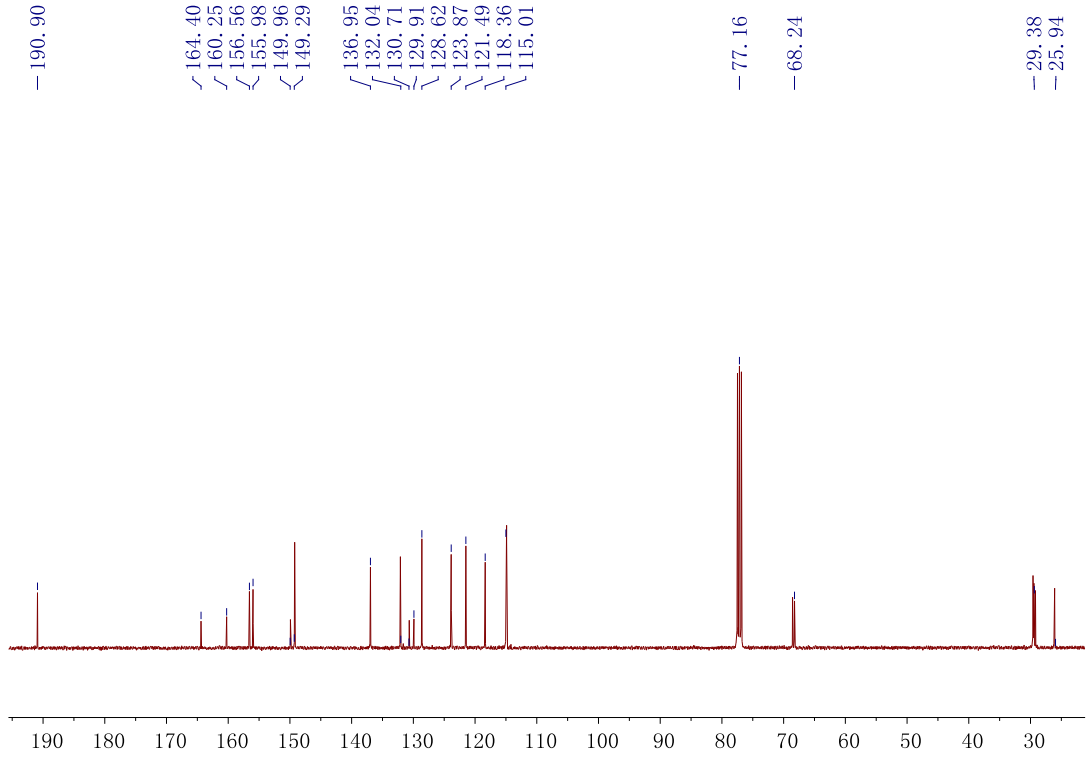

Figure S2. ^{13}C NMR spectrum (75 MHz, $CDCl_3$, room temperature) of compound **8**.

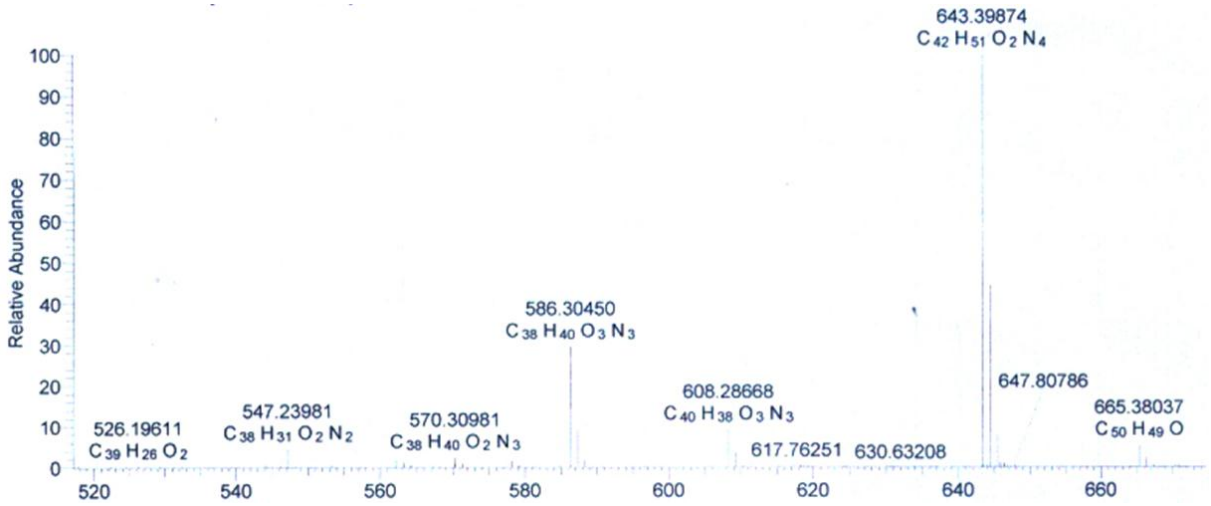

Figure S3. Electrospray ionization mass spectrum of compound **8**.

*2.2 Synthesis of compound **1***

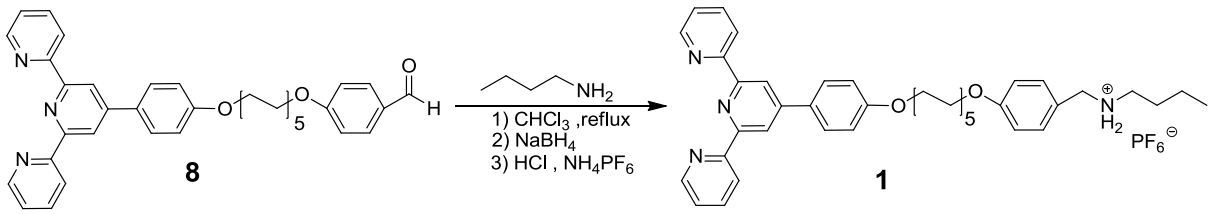

Compound **8** (2.60 g, 4.34 mmol) and *n*-butylamine (0.95 g, 13.0 mmol) were refluxed in $CHCl_3$ (40 mL) for 16 h. After the reaction was cooled down to room temperature, $CHCl_3$ was removed with a rotary evaporator and the residue was redissolved in methanol (80 mL). $NaBH_4$ (0.82 g, 21.70 mmol) was then added and the resulting mixture was stirred for 10 h at room temperature. Subsequently, the solvent was removed with a rotary evaporator and the residue was extracted with H_2O/CH_2Cl_2. Then, the combined organic extracts were removed with a rotary evaporator. The residue was purified by flash column chromatography (dichloromethane/methanol, 20 : 1 *v/v* as the eluent) to afford the amine as a pale yellow liquid. The amine was stirred with 3 M HCl (10 mL) in methanol for 1 h, and NH_4PF_6 (0.76 g, 4.67 mmol) was subsequently added. The reaction mixture was stirred for 5 h at room temperature. Excess HCl and NH_4PF_6 were destroyed with H_2O. Methanol was removed with a rotary evaporator and the residue was filtered to provide compound **1** as a white solid (1.54 g, 45%). Mp: 198.8–200.1 °C. The ^{1}H NMR spectrum of compound **1** is shown in Figure S4.

^{1}H NMR (300 MHz, CD_3CN, room temperature) δ (ppm): 8.78 (d, 2H), 8.48 (d, 2H), 8.44 (s, 2H), 8.00 (m, 2H), 7.86 (d, 2H), 7.51 (m, 2H), 7.10 (m, 4H), 6.65 (d, 2H), 4.10 (m, 2H), 4.06 (s, 2H), 3.73 (m, 2H), 3.13 (m, 2H), 1.80 (m, 2H), 1.69 (m, 2H), 1.57 (m, 2H), 1.51 (m, 2H), 1.41 (m, 2H), 1.39 (m, 2H), 1.30 (m, 8H), 0.90 (m, 3H). The ^{13}C NMR spectrum of compound **1** is shown in Figure S5. ^{13}C NMR (75 MHz, DMSO-d_6, room temperature) δ (ppm): 156.0, 159.2, 155.6, 155.1, 149.3, 148.9, 137.4, 131.4, 129.4, 128.1, 124.4, 123.5, 120.9, 117.2, 115.2, 114.5, 67.5, 49.6, 46.0, 28.9, 28.7, 28.6, 27.4, 25.4, 19.2, 13.4. ESI–MS m/z: [M – PF_6]$^{+}$ calcd for $C_{42}H_{51}N_4O_2$, 643.4007; found, 643.3997; error, 1.6 ppm.

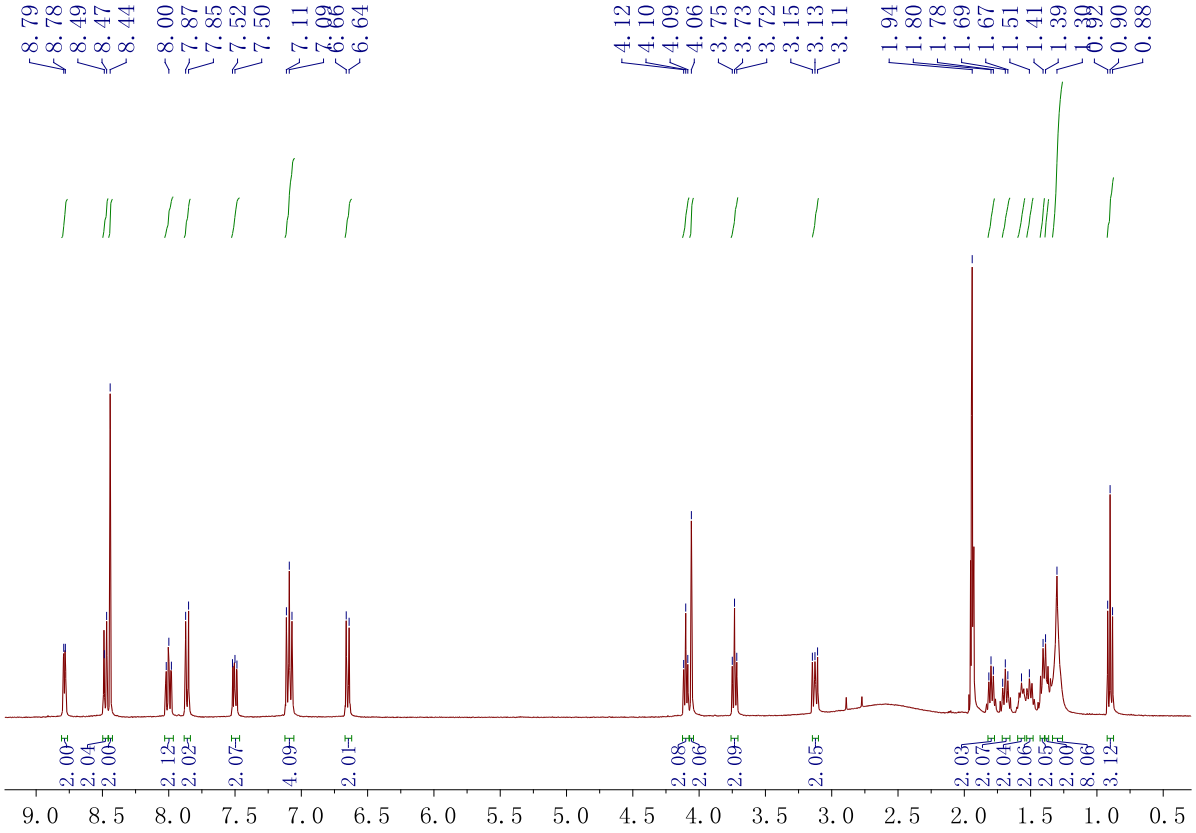

Figure S4. ^{1}H NMR spectrum (300 MHz, CD_3CN, room temperature) of compound **1**.

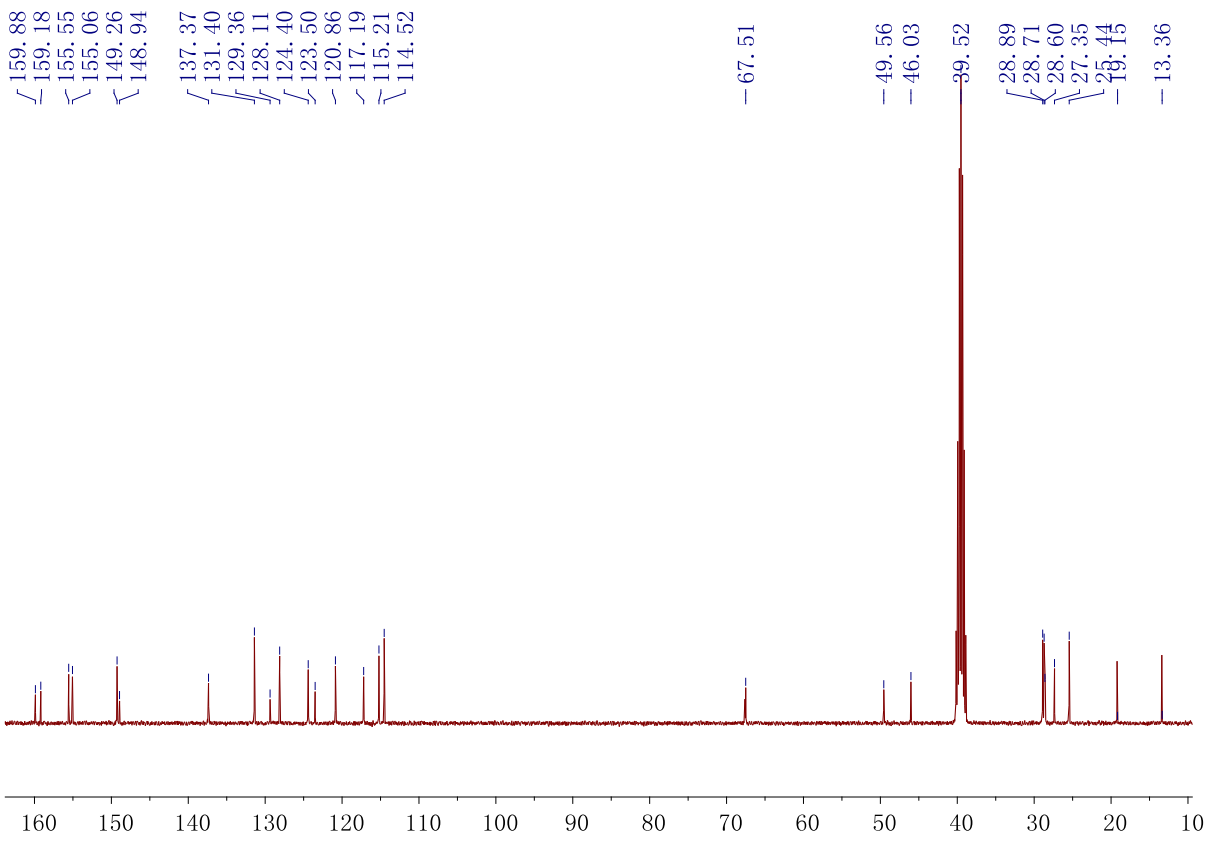

Figure S5. ^{13}C NMR spectrum (100 MHz, DMSO-d_6, room temperature) of compound **1**.

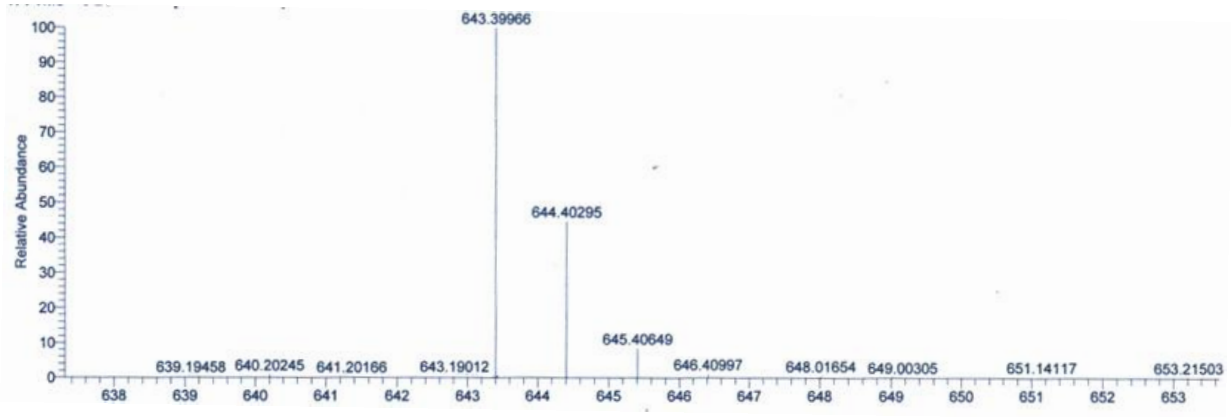

Figure S6. Electrospray ionization mass spectrum of compound **1**.

*2.3 Synthesis of compound **2***

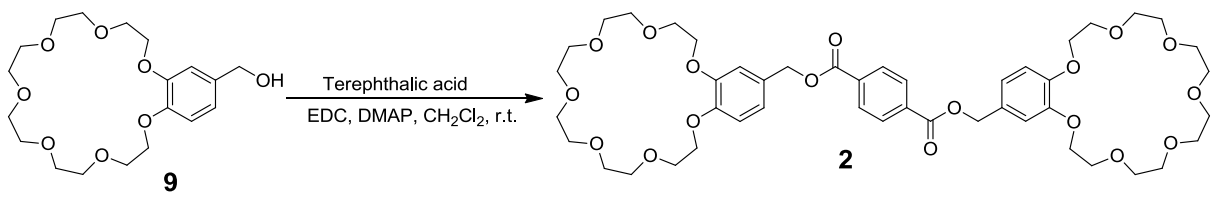

A solution of terephthalic acid (0.187 g, 1.13 mmol), EDC·HCl (0.691 g, 3.62 mmol)

and DMAP (0.110 g, 0.90 mmol) in dichloromethane (100 mL) was stirred for 1 h at room temperature, and then compound **9** (1.00 g, 2.59 mmol) was added. The reaction mixture was stirred for 24 h at room temperature, filtered, washed with brine and then dried on $MgSO_4$. The solvent was removed in *vacuo* and the crude product was purified by flash column chromatography (dichloromethane/methanol, 20 : 1 *v/v* as the eluent) to provide **2** as a white solid (0.59 g, 50%).[S3] Mp: 101.6–103.2 °C. The ^{1}H NMR spectrum of compound **2** is shown in Figure S7. ^{1}H NMR (300 MHz, $CDCl_3$, room temperature) δ (ppm): 8.10 (s, 4H), 6.99 (d, 4H), 6.88 (d, 2H), 5.28 (s, 4H), 4.17 (m, 8H), 3.93 (m, 8H), 3.56–3.83 (m, 32H).

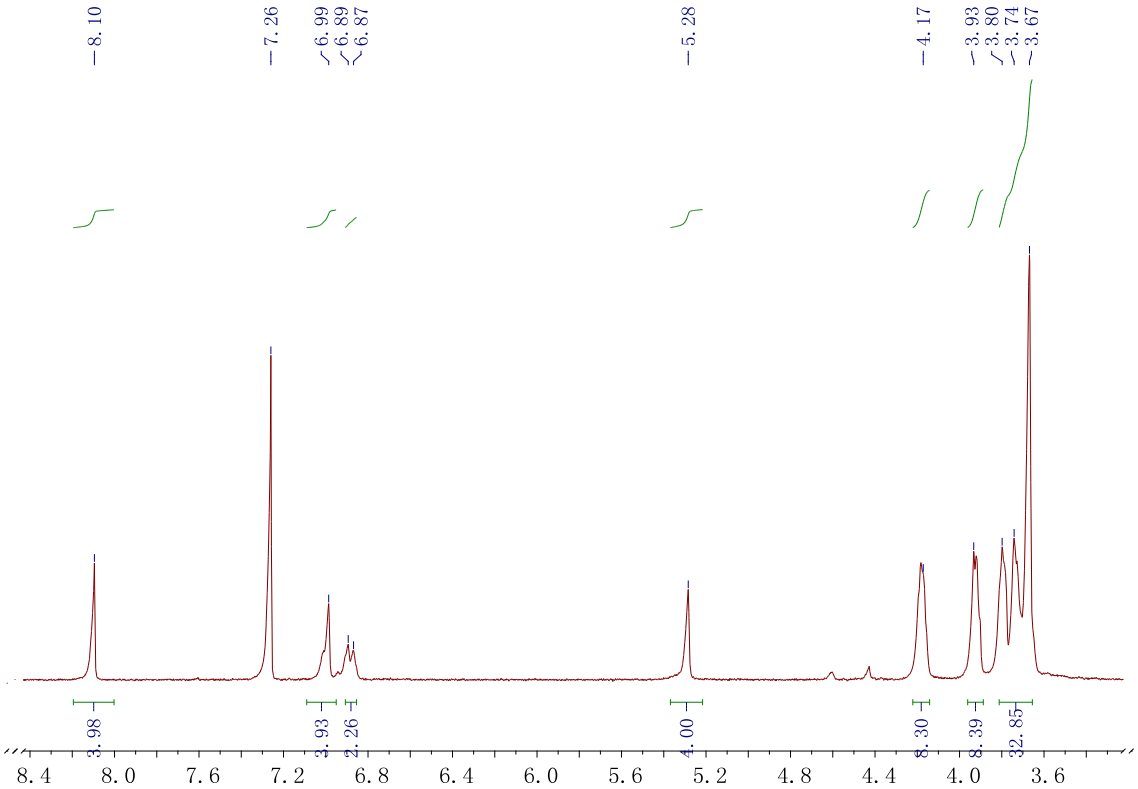

Figure S7. ^{1}H NMR spectrum (300 MHz, $CDCl_3$, room temperature) of compound **2**.

*3. ^{1}H NMR complexation between compounds **1** and **2***

As shown in Figure S8, ^{1}H NMR spectrum of 2 : 1 mixture of compounds **1** and **2** exhibits three sets of signals for the protons belonging to B21C7/secondary ammonium salt recognition motif, corresponding to the uncomplexed host, uncomplexed guest, and complexed host–guest molecules, which stands for slow-exchange complexation between the

B21C7 and secondary ammonium salt moieties on the ^{1}H NMR time scale. After the formation of [3]pesudorotaxane structure, the complexed aromatic protons $H_{10–11}$ and methylene protons H_{12} on **1**, as well as the ethyleneoxy protons $H_{19–20}$ on **2**, move downfield significantly. The obvious proton chemical shifts definitely support that the secondary ammonium salt moiety NH_2^+ is located in the center of the B21C7 macrocyclic ring. On the other hand, no obvious chemical shift changes occur for the terpyridine unit, demonstrating the preferential host–guest complexation without the involvement of terpyridine ligand.

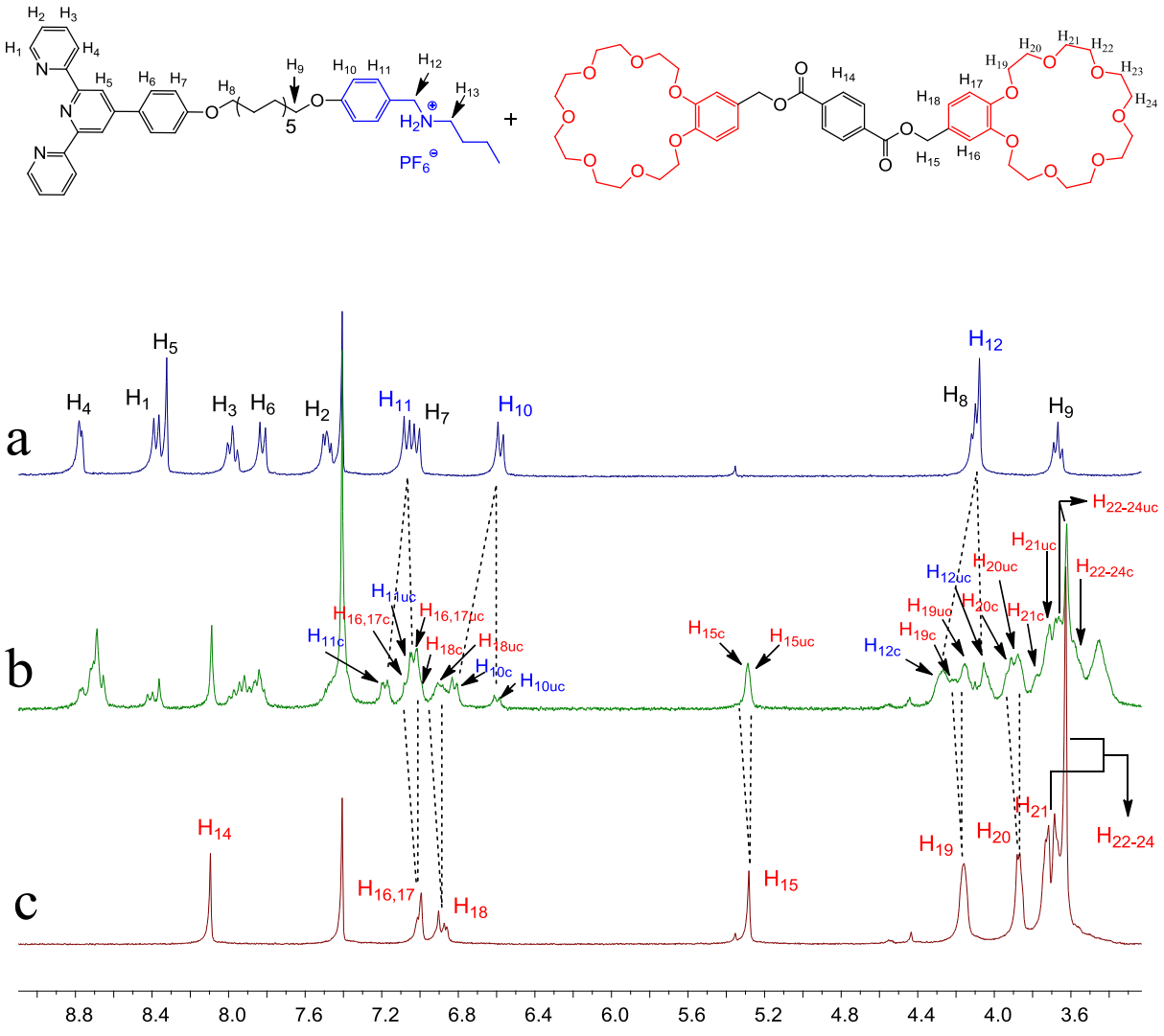

Figure S8. Proton NMR spectra (300 MHz, $CDCl_3/CD_3CN$ (3/1, *v/v*), 25 °C) of (a) 8.00 mM **1**, (b) 1 : 2 equimolar mixture of 4.00 mM **1** and 8.00 mM **2**, and (c) 8.00 mM **2**. All of these chemical shift changes indicate that the B21C7 rings of **2** are complexed by the secondary ammonium salts on **1** to form the [3]pseudorotaxane structure. Peaks associated with the complexed and uncomplexed crown ether and secondary ammonium salts are designated by

(c) and (uc), respectively.

*4. UV/Vis titration between $Zn(OTf)_2$ and compound **1***

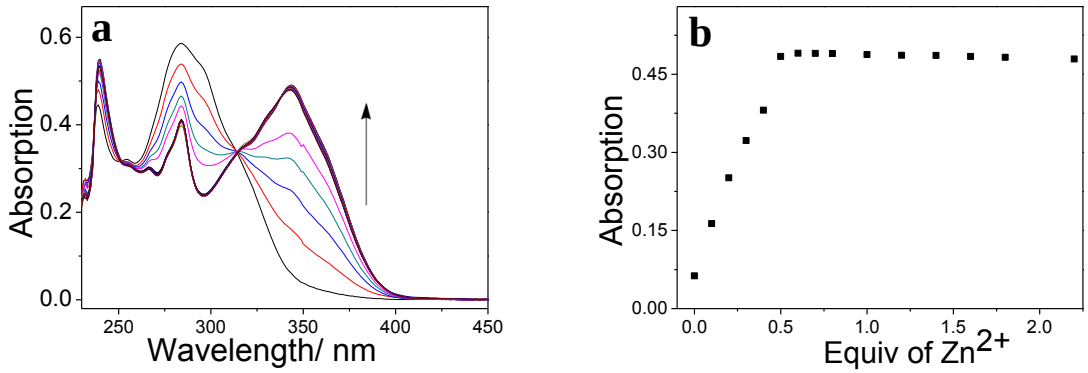

Figure S9. Change in the UV/Vis absorption spectra upon stepwise addition of $Zn(OTf)_2$ (1.0 mM in $CHCl_3/CH_3CN$ (3/1, *v/v*)) to a 0.02 mM solution of monomer **1** in $CHCl_3/CH_3CN$ (3/1, *v/v*). a) UV/Vis absorption spectra. b) The normalized absorbance at 343 nm. The formation of metal–ligand complex was evidenced by a clear isobestic point at 315 nm, indicating the efficient conversion from free to metal–complexed terpyridine species. The achievement of maximum absorbance (λ_{max} = 343 nm) at the $Zn(OTf)_2$/**2** molar ratio of 0.5 apparently supports the formation of $Zn(tpy)_2^{2+}$ complex.

*5. UV/Vis titration between $Zn(OTf)_2$ and 2 : 1 mixtures of monomers **1** and **2***

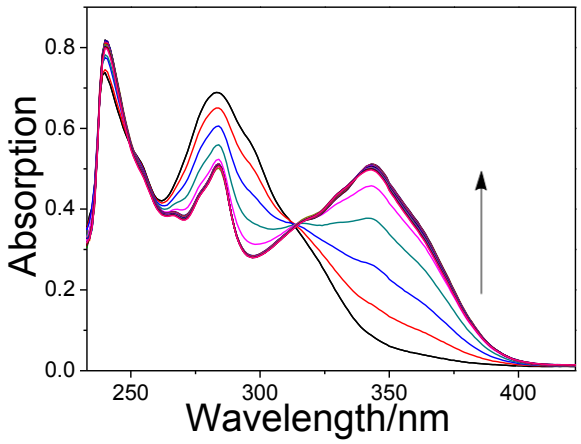

Figure S10. Change in the UV/Vis absorption spectra upon stepwise addition of $Zn(OTf)_2$ to 2 : 1 mixtures of monomers **1** and **2** in $CHCl_3/CH_3CN$ (3/1, *v/v*). The formation of metal–ligand complex was confirmed by a clear isobestic point at 315 nm, indicating the efficient

conversion from free to metal–complexed terpyridine species.

*6. ^{1}H NMR titration between Zn(OTf)$_2$ and monomer **1***

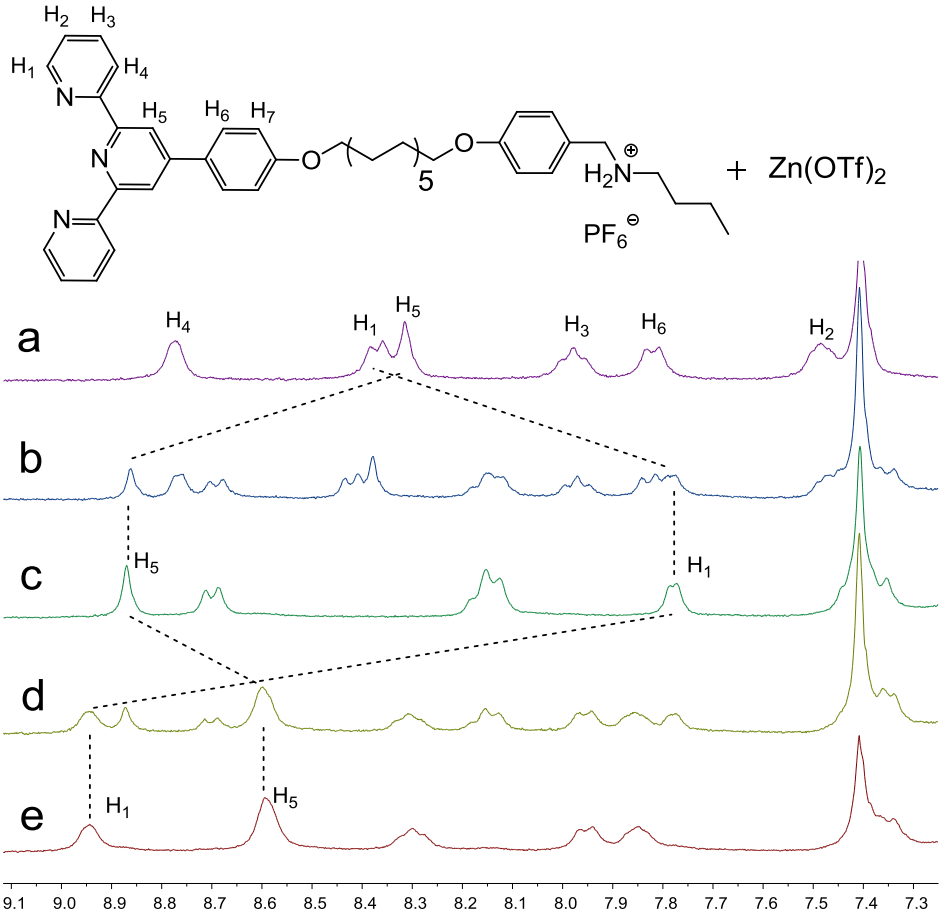

Figure S11. Partial ^{1}H NMR spectra (300 MHz, $CDCl_3/CD_3CN$ (3/1, v/v), 25°C) of monomers **1** (4.0 mM) upon gradual addition: (a) 0; (b) 0.2; (c) 0.5; (d) 0.8; (e) 1.5 equiv. of $Zn(OTf)_2$. When the feed-ratio of Zn^{2+}/tpy is 0.5, original uncomplexed signals totally disappear, representing the formation of dimeric $Zn(tpy)_2^{2+}$ complex. However, once Zn^{2+}/terpyridine ratio is further increased to 3 : 2, a third set of signals evolve and gradually strengthen, along with the disappearance of $Zn(tpy)_2^{2+}$ signals, suggesting the formation of 1 : 1 metal–ligand complex $Zn(tpy)^{2+}$. Such results demonstrate kinetically labile property of Zn^{2+}–terpyridine complex.

*7. Concentration-dependent ^{1}H NMR measurements among Zn(OTf)$_2$, monomers **1** and **2***

Concentration-dependent ^{1}H NMR measurements was performed to evaluate the monomer concentration effect on the formation of linear supramolecular polymers **5**. Upon

mixing 1 : 2 : 1 molar ratio of $Zn(OTf)_2$, **1** and **2** in $CDCl_3/CD_3CN$ (3/1, *v/v*) at low concentration, well-defined signals for B21C7–secondary ammonium salt moieties in ^1H NMR spectra indicate the domination of cyclic oligomers. As the monomer concentration gradually increases, the original cyclic benzylic protons H_{15} and ethyleneoxy protons of B21C7 unit progressively decrease, whilst the newly formed linear species gradually strengthen, revealing the formation of high-molecular-weight aggregates at high concentration. On the other hand, complete complexation of terpyridine ligand with Zn^{2+} could be observed for all the measured concentrations, consistent with the UV/Vis titration results. Moreover, the terpyridine signals remain almost unchanged between cyclic oligomers and linear supramolecular polymers, presumably due to the similar environment for these two species.

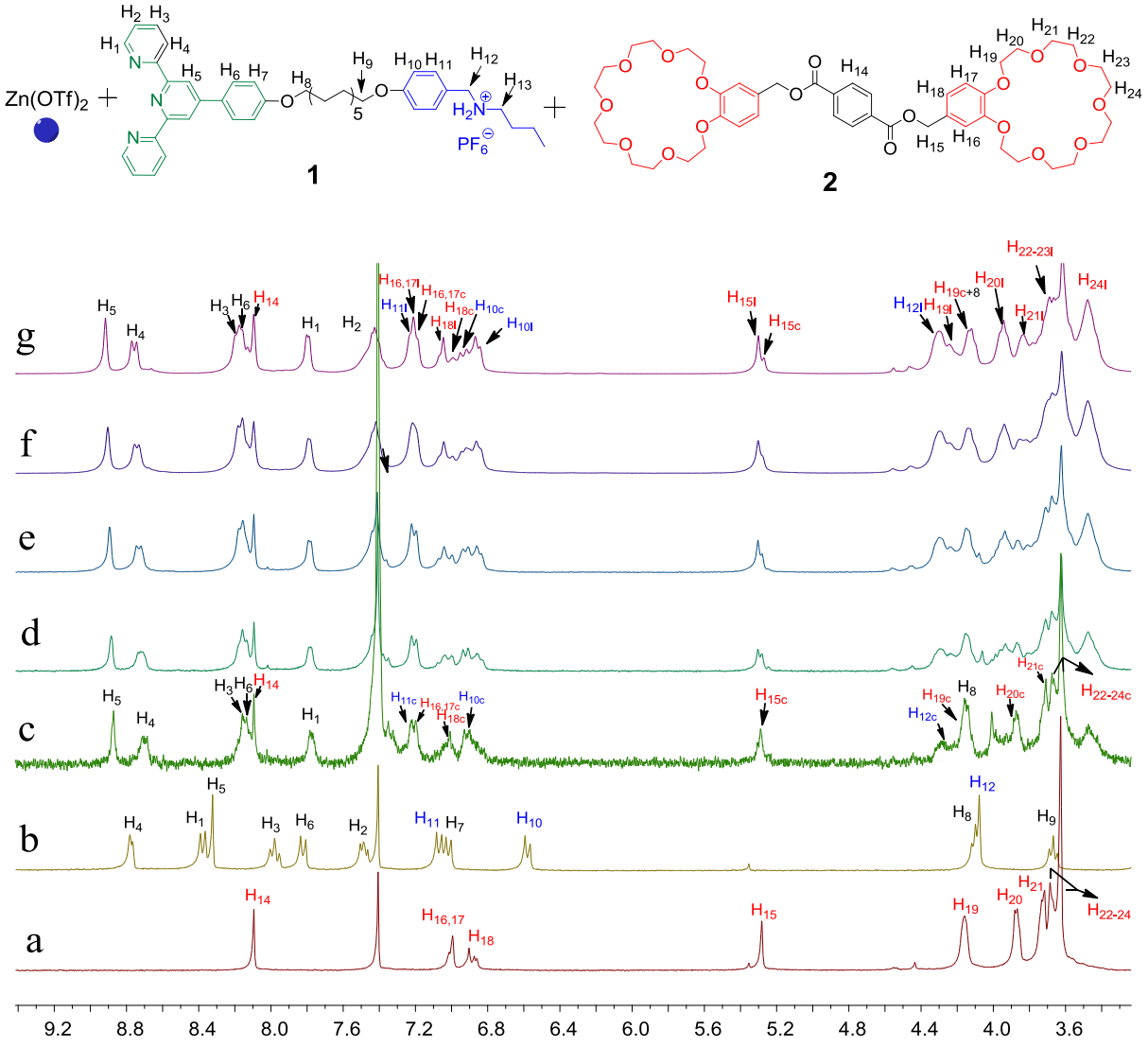

Figure S12. Partial ^1H NMR spectra (300 MHz, $CDCl_3/CD_3CN$ (3/1, *v/v*), 25 °C) of (a) **2**; (b)

1; 1 : 2 : 1 molar ratio of $Zn(OTf)_2$, **1** and **2** at different terpyridine concentrations: (c) 0.02; (d) 0.04; (e) 16.2; (f) 51.4; (g) 111 mM. Here ‘‘c’’ and ‘‘l’’ denote cyclic and linear species, respectively.

*8. DOSY spectra of supramolecular polymers **5** at different monomer concentrations*

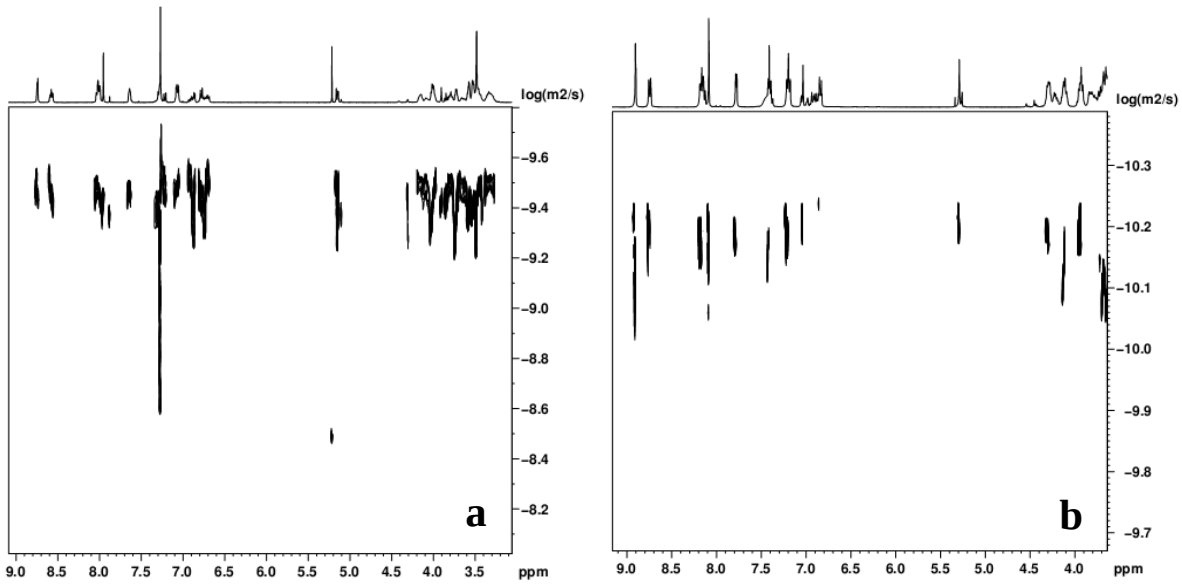

Figure S13. Two-dimensional diffusion-ordered NMR (DOSY) spectra of 1 : 2 : 1 molar ratio of $Zn(OTf)_2$, **1** and **2** in $CDCl_3/CD_3CN$ (3/1, *v*/*v*) at different concentrations: (a) 4.00 mM; (b) 80.0 mM. The measured diffusion coefficients decreased considerably from 3.57×10^{-10} to 6.37×10^{-11} m^2 s^{-1} from 4.00 mM to 80.0 mM, confirming the formation of high-molecular-weight aggregates at high concentration.

*9. Viscosity measurement of supramolecular polymers **5** at different monomer concentrations*

Macroscopic properties of the resulting supramolecular assemblies were investigated by capillary viscosity measurements. For the linear supramolecular polymer **5** derived from 1 : 2 : 1 molar ratio of $Zn(OTf)_2$, **1** and **2**, double logarithmic plots of specific viscosity *versus* concentration exhibited a clear slope change (Figure S14). In the low concentration range, the slope value was 1.12, characteristic of the presence of cyclic oligomers with constant size.

With increasing concentration, a clear rise in the viscosity was observed (slope = 1.70). The stronger concentration dependence indicated the formation of supramolecular polymers of increasing size. Moreover, the CPC value was determined from the onset of the steeper portion, yielding a value of 9 mM. The relatively low CPC value for the supramolecular polymerization process could be attributed to the length mismatch effect of the two monomers, which significantly suppress the propensity to form cyclic species.

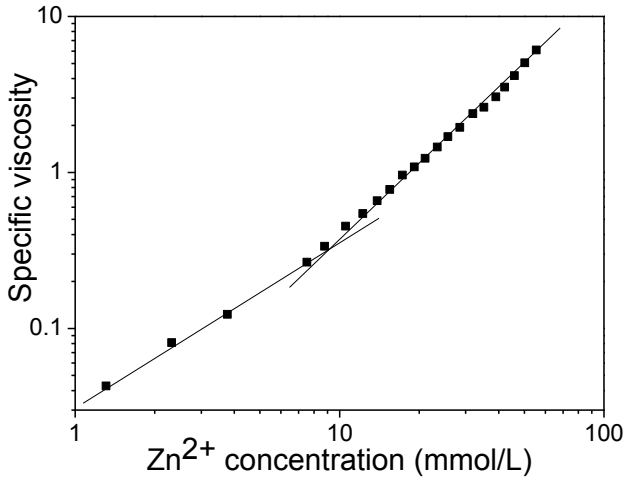

Figure S14. Specific viscosity of the linear supramolecular polymer **5** as a function of concentration.

*10. UV/Vis titration of cyclen and Zn(OTf)$_2$ to supramolecular polymers **5***

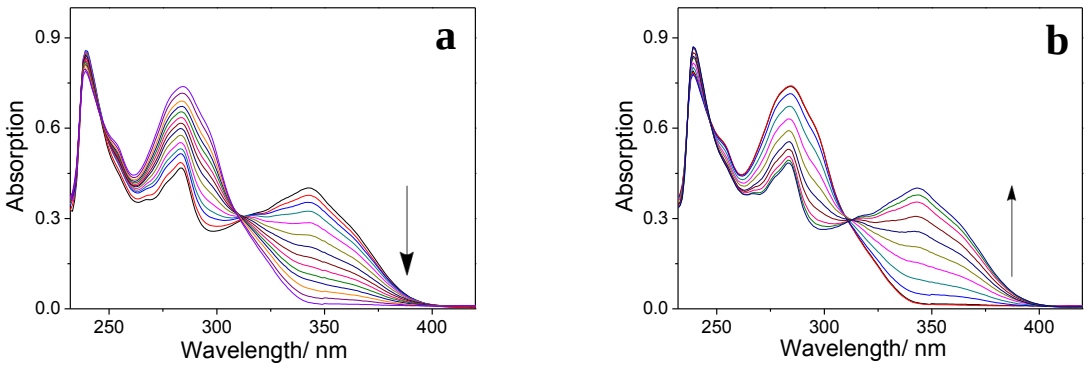

Figure S15. Change in the UV/Vis absorption spectra: (a) stepwise addition of competitive ligand cyclen to a 1 : 2 : 1 mixture of Zn(OTf)$_2$, **1** and **2** in $CHCl_3/CH_3CN$ (3/1, *v/v*); (b) subsequent addition of Zn(OTf)$_2$ to the above solution. Adding 4 equiv. of cyclen results in the total disappearance of Zn^{2+}/tpy absorption bands (λ_{max} = 343 nm). Moreover, reformation of

supramolecular polymers **5** could be achieved *via* the addition of equal amounts of $Zn(OTf)_2$, as verified by the reappearance of Zn^{2+}/tpy absorption band.

References:

S1. Anthonysamy, A.; Balasubramanian, S.; Shanmugaiah, V.; Mathivanan, N. *Dalton Trans.* **2008**, *16*, 2136.

S2. Marx, V. M.; Girgis, H.; Heiney, P. A.; Hegmann, T. *J. Mater. Chem.* **2008**, *18*, 2983.

S3. Chen, L.; Tian, Y.-K.; Ding, Y.; Tian, Y.-J.; Wang, F. *Macromolecules* **2012**, *45*, 8412.